

Kinetic phase diagrams of a ternary hard sphere mixture

A. Vizcarra-Rendón¹, A. Puga-Candelas¹, S. Aranda-Espinoza¹, M. A. Chávez-Rojo², and R. Juárez- Maldonado¹

¹Unidad Académica de Física, Universidad Autónoma de Zacatecas,
Calzada Solidaridad Esquina con Paseo la Bufa S/N, C.P. 98060 Zacatecas, Zac., México.

²Facultad de Ciencias Químicas, Universidad Autónoma de Chihuahua. Circuito No. 1,
Nuevo Campus Universitario; Chihuahua, Chuh. México.

(Dated: August 26, 2019)

We use the Self Consistent Generalized Langevin Equation theory (SCGLE) to study the dynamic arrest transitions of a system of three species of hard sphere colloidal system in the size ratio 1:3:9. We find that the inclusion of the smallest species has a depletion effect that drives the system to a second glass-liquid-glass re-entrance in a similar way that the inclusion of a small species in an otherwise monodisperse system leads to a (first) re-entrance. And we also find that the new glass after the second reentrance has very small localization length. Additionally we compare the kinetic phase diagram of a binary hard sphere mixture with size asymmetry 1:5, obtained with Mode Coupling Theory (MCT) and SCGLE theory and exhibit the significant differences between the two theories..

kinetic phase diagram, dynamic arrest, hard-spheres
4.70.pv,64.70.P-

PACS numbers: 6

INTRODUCTION

A lot of study has been devoted to the understanding of the glass transition due to its theoretical, fundamental and technological importance [1]. These meta-stable states can be found in both simple and colloidal fluids[2]. Colloidal systems offer, however, the unique opportunity to tailor the interaction potential between the particles, and the time scale, being much longer, allows an easier study of such systems, from the experimental stand point [3–9].

The foremost theoretical formalism to account for much of the experimental work done so far is the Mode-Coupling (MC) approach [10]. One of the most impressive predictions of this theory was the glass-liquid-glass re-entrant transition in hard-spheres colloidal fluids [11, 12]. The theory nonetheless yields conflicting answers when a bidisperse system [8, 9] is treated as it is, i.e. a true bidisperse system, and as compared with an effective one-component fluid under the MC approach [13]. Recently, however, a theory that seems to be better suited to the study of these systems, mainly in multicomponent case, has been put forward [14, 15]. We henceforth refer to it as the self-consistent generalized langevin equation (SCGLE) theory.

On the hand of simulations experiments there is several attempts of investigate the static and dynamic properties of hard sphere mixtures. Particularly have made studies of the dynamics of polydisperse systems, by however, none has achieved the kinetic phase diagrams.

The importance of the study of colloidal mixtures is crucial to the understanding of the dynamic properties of polydisperse systems, because there is not monocomponent ideal system in the nature. Especialy, for simplicity, the case of two and three species is fundamental to understand the more basic properties of such systems. Specifically the clasification of the different types of phases that may occur is fundamentally important. That classification can be drawn in what is known as kinetic phase diagram. Particularly the topology of the diagram such as we will see, say a lot about the different states of the system.

In this work, we use SCGLE theory to analyze the likelihood of getting a second "re-entrant" transition when a smaller particle species is introduced into a bidisperse system. Thus the system that we are envisioning is a three component mixture of hard spheres with size asymmetry, namely, hard spheres of relative sizes 1, 3 and 9, which we will refer to as 1 : 3 : 9. And with help of the localization length we can catalog the differents types of phases of the system.

SCGLE THEORY FOR DYNAMIC ARREST

The SCGLE theory of dynamic arrest was introduced in Refs. [16–19] and extended to colloidal mixtures in Ref. [14]. The relevant dynamic information of an equilibrium ν -component colloidal suspension is contained in the $\nu \times \nu$ matrix $F(k, t)$ whose elements are the *partial intermediate scattering functions* $F_{\alpha\beta}(k, t) \equiv \langle n_{\alpha}(\mathbf{k}, t) n_{\beta}(-\mathbf{k}', 0) \rangle$,

where $n_\alpha(\mathbf{k}, t) \equiv \sum_{i=1}^{N_\alpha} \exp[i\mathbf{k} \cdot \mathbf{r}_i(t)]/\sqrt{N_\alpha}$, with $\mathbf{r}_i(t)$ being the position of particle i of species α at time t . The initial value $F_{\alpha\beta}(k, 0)$ is the partial static structure factor $S_{\alpha\beta}(k)$ [20, 21]. The SCGLE theory is summarized by a self-consistent system of equations [14, 22] for the $\nu \times \nu$ matrices $F(k, t)$ and $F^{(s)}(k, t)$. The latter being defined as $F_{\alpha\beta}^{(s)}(k, t) \equiv \delta_{\alpha\beta} \langle \exp[i\mathbf{k} \cdot \Delta\mathbf{R}^{(\alpha)}(t)] \rangle$, where $\Delta\mathbf{R}^{(\alpha)}(t)$ is the displacement of any of the N_α particles of species α over a time t , and $\delta_{\alpha\beta}$ is Kronecker's delta function. As illustrated in Ref. [14], the solution of the SCGLE theory above provides the time and wave-vector dependence of the main dynamic properties. It also provides equations for their long-time asymptotic values, referred to as non-ergodicity parameters, which play the role of order parameters for the ergodic–non-ergodic transitions. The most fundamental of these results [14] is the following equation for the asymptotic mean squared displacement $\gamma_\alpha \equiv \lim_{t \rightarrow \infty} \langle (\Delta\mathbf{R}^{(\alpha)})^2 \rangle$,

$$\frac{1}{\gamma_\alpha} = \frac{1}{3(2\pi)^3} \int d^3k k^2 \{ \lambda[\lambda + k^2\gamma]^{-1} \}_{\alpha\alpha} \times \{ c\sqrt{n}S\lambda[S\lambda + k^2\gamma]^{-1}\sqrt{n}h \}_{\alpha\alpha}, \quad (1)$$

where S is the matrix of partial static structure factors, h and c are the Ornstein-Zernike matrices of total and direct correlation functions, respectively, related to S by $S = I + \sqrt{n}h\sqrt{n} = [I - \sqrt{n}c\sqrt{n}]^{-1}$, with the matrix \sqrt{n} defined as $[\sqrt{n}]_{\alpha\beta} \equiv \delta_{\alpha\beta}\sqrt{n_\alpha}$, and $\lambda(k)$ is a diagonal matrix given by $\lambda_{\alpha\beta}(k) = \delta_{\alpha\beta}[1 + (k/k_c^{(\alpha)})^2]^{-1}$, where $k_c^{(\alpha)}$ is the location of the first minimum following the main peak of $S_{\alpha\alpha}(k)$ (a more practical rule is to use simply $k_c^{(\alpha)} = 1.545(2\pi/\sigma_\alpha)$, with σ_α the diameter of species α). The solution of Eq. 1 give us the criterion to determine when a species is arrested or not, namely, if $\gamma_\alpha \rightarrow \infty$ the species α is in a fluid state and if γ_α is finite then it is in arrested state; particularly $\sqrt{\gamma_\alpha}$ is its localization length.

THE SYSTEM DESCRIPTION

Let a three component hard-sphere-like colloidal system be composed of N particles with three different species (A,B,C) of which N_A are of diameter σ_A , N_B of σ_B and N_C of σ_C and $N = N_A + N_B + N_C$. For simplicity, we will consider the case where $\sigma_A = 9$, $\sigma_B = 3$ and $\sigma_C = 1$. The control parameters will be the volume fractions ϕ_A, ϕ_B and ϕ_C of the species A, B and C respectively; where $\phi_\alpha = \pi n_\alpha \sigma_\alpha^3/6$, with $n_\alpha = N_\alpha/V$ and V is the volume of the system. The size asymmetry parameter $\delta_{(ij)} = \sigma_i/\sigma_j$ can be useful. We have numerically resolved the Eq. (1) for the above system and calculated its full dynamic arrest phase diagram. In calculation of the matrix of partial static structure factors needed to resolve the Eq. (1) we have used the analytical Baxter [23] solution of Ornstein-Zernike equations with Percus-Yevick approximation for a multicomponent hard sphere system.

RESULTS

To describe the dynamic arrest transitions of a ternary hard sphere mixture we need a three dimensional cartesian space, is to say, the space (ϕ_A, ϕ_B, ϕ_C) . The results are as follows:

The (ϕ_A, ϕ_B) plane

We start by showing the dynamic arrest phase diagram (Fig. 1) for the case in which the species C (smaller) is found at infinite dilution. The red curve represents the line of arrest for the large particles; below and the left of it the large particles are found in liquid state, while above of it lies the region of arrested states. The interception of this line with the ϕ_A axis represents the arrest of the large particles when there are no other particles (monocomponent glass transition point), which happens at the volume fraction of $\phi_A = 0.537$. As we increase the volume fraction of species B, the lines move to the right due to the effect of depletion forces as discussed elsewhere [15, 24]. The red line moves to approximately $\phi_A = 0.554$ where it joints the dashed black line (line of arrest of the middle species, see zoom Fig. 2), and after that both lines move together to the left, making a curve of simultaneous arrest of species A and B. Between the red curve and the black curve we find mixed states where particles A remain arrested but particles B are moving in an ergodic state. The nature of this hybrid states can be undersood because the species A reached the ideal glass transition, and the presence of species B and C (which continues to spread) only shifts the transition point. As we increase the volume fraction of species A, the accessible volume to the species B is getting smaller until eventually

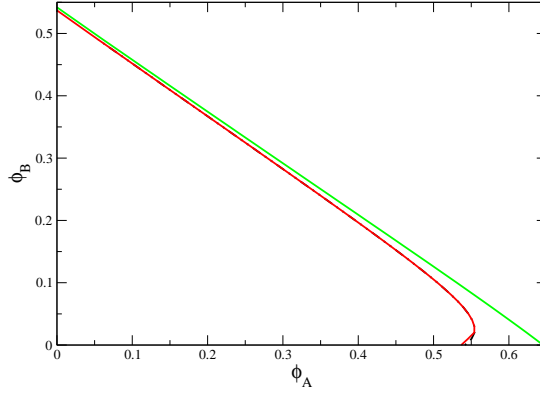


FIG. 1: Dynamic arrest phase diagram of a ternary hard sphere mixture with $\phi_C = 0$. The red line represents the transition of species A from fluid state to an arrested state, the dotted line indicates the virtual localization of species B, and the green dashed line corresponds to the localization transition of particles C

it is located. We also show a green line, representing the line of arrest for the small particles, which are found at infinite dilution through out this graph, i.e., there remains just a trace of them. Thus above the green curve and to its right all particles are found in the glass, non-ergodic state, while between lines we have corresponding mixed states. The crossings of these lines with the ϕ_A axis represent the sequential arrest of the A, B and C species found at the following volume fractions of the third species: $\phi_A = 0.537, 0.542$ and 0.645 . If we disregard the green line (the line of arrest for species C), what we get is the same kind of diagram reported elsewhere for binary hard-sphere mixture [15]. In contrast with the two component system, we now have the possibility of having two kinds of arrested species, A and B, and the C species moving in the porous medium formed by the matrix of obstacles created by the arrest of species A and B. This is the region of states between the green and red curves.

First re-entrance

An interesting phenomenon already discussed in the case of the bidisperse system is the re-entrance in the kinetic phase diagram, whereby we mean the following: consider a two-component system whose state is represented by a point in the ϕ_A axis at volume fraction of, say, $\phi_A = 0.54$; at this volume fraction the species A is already arrested (lower dot in Fig. 2). If we now increase the volume fraction of the species B, we move upwards in this phase diagram. By doing

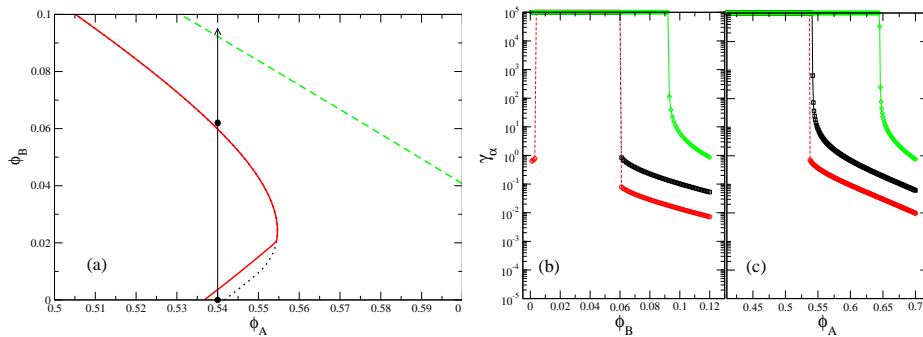


FIG. 2: (a) This is a close up of Fig. 1. The lower point represent a mixed state where particles A are arrested while the B and C are moving. The upper point is an state where the particles A and B are arrested while the C are diffusing. (b) Shows the square of localization length of specie A (red), specie B (black) and specie C (green); calculated along the arrow indicated in Fig2a. (c) Square of localization length but now along the axis ϕ_A , i.e., with only a trace of species B and C. In all cases the units of localization length of specie α is its own diameter σ_α . And the top numeric label (10^5) of vertical axis in (b) and (c) is a representation of infinity, i.e., the localization length is infinite (particles in a fluid state.)

This effect is due to the depletion forces caused by the B particles, whereby the A particles feel an attraction of the Asakura-Oosawa [24] type and get closer together, which makes room for the particles to move; in other words, since the cages open up, the system melts. Not only is there more room for the large particles but for all particles as well, as can be inferred by the fact that all lines start moving to the right. If we still continue to increase the volume fraction of particles B, we arrive at a total volume fraction in which both species get arrested, this is represented by the upper dot in Fig. 2. From the point of intersection, both lines (black and red) merge into one up to the left extreme where $\phi_A = 0$, here the arrest of the species B arrests the large ones, since there are no holes through which they can go through. The particles C, however, still have some room and at this extreme they get arrested when $\phi_B = 0.542$. As we can see from Fig. 2, there is a gap between the green and red-black lines that do not intersect even when the volume fraction of the species A (the larger particles) vanishes. And what happens is this: when we have no A and C species, the species B gets arrested at the volume fraction of $\phi_B = 0.537$, and the trace of species A is arrested by the particles B. The species C gets arrested at the expected value of $\phi_C = 0.542$, since at this end on the phase diagram, where $\phi_C = 0$, the system is equivalent to a bidisperse system with a size asymmetry of $\delta_{(BC)} = \sigma_B/\sigma_C = 0.333$; then we have to recover the same values of arrest found in the ϕ_A axis by the black(arrest of particles B) and red lines(arrest of particles A), since $\delta_{(AB)} = \delta_{(BC)} = 0.333$.

On the other hand, at small volume fractions of the species B, the glass is due to the cage effect and we call it *repulsive glass* [8, 15]. However at higher volume fractions of it, the glass formed by the large particles is of a different type. This part of the diagram is called *attractive glass* [8, 15], since what we see, disregarding the presence of the particles B, that there is an effective attraction among the particles of type A, and the localization length of particles B becomes smaller than particles B on the first part of the curve by two orders of magnitude. If we continue along this line to smaller volumes fractions of the particles A until only a trace of them is found we have the "*chancaquilla effect*" [14], where the particles A are arrested because the particles B get arrested. For intermediate volume fractions of the particles A, they get arrested because of the combined effect of the volume fractions; that is, due to the total volume fraction (at this size as

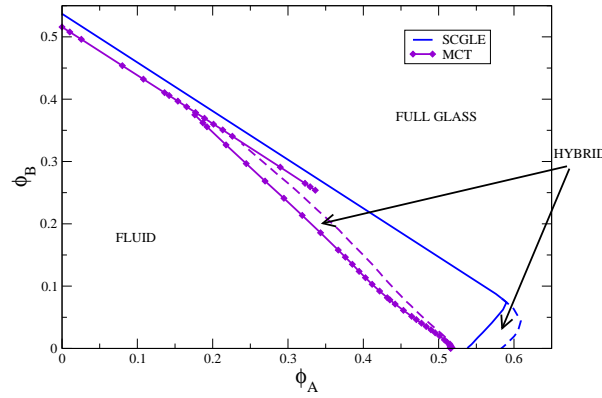


FIG. 3: Quantitative comparison between the dynamic arrest diagrams of MCT theory (violet symbol-line) and SCGLE theory (blue line). In both diagrams are distinguished three regions: fluid, full glass and partial (hybrid) glass states. Note that MCT theory does not show reentrant effect.

Second re-entrance

In the discussion of the previous section, the species C has played no active role since it was found at infinite dilution. Our system was essentially a two-component system. However, we have three species, so the phase diagram is actually tridimensional. Up to now, we have shown only the (ϕ_A, ϕ_B) axis slice of the three-dimensional phase space when $\phi_C = 0$. We will now increase the volume fraction of species C, i.e., we will move along the ϕ_C axis and show different slices at different values of the volume fraction of the particles C. The next slice that we show corresponds to $\phi_C = 0.05$ in Fig. 4. Note that the lines move to the right, once more as a consequence of depletion forces. This causes a second re-entrance, but this time due to the addition of particles C. The black dot has the same coordinates as that in Fig. 2 and, as we can see, this point finds itself in the ergodic region. Note also that this time the arrest lines of particle A and B merge at around $\phi_3 = 0.595$. And if we continue increasing the volume fraction of species

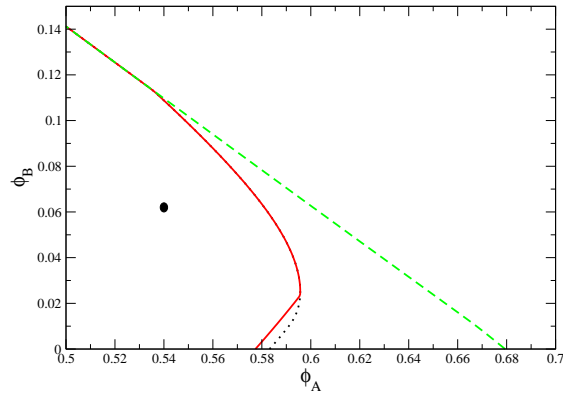


FIG. 4: Here we show the $\phi_C = 0.05$ plane. Note that the arrest lines moved to the right, and this time all lines merge at some point. The dot shown is inside the ergodic region and correspond to the dot in Fig. 2.

C, we do indeed get arrested again, Fig. 5. This time all particles are arrested, as we can see. Here the three lines have merged into one, and the glass transition occurs in the non-ergodic region.

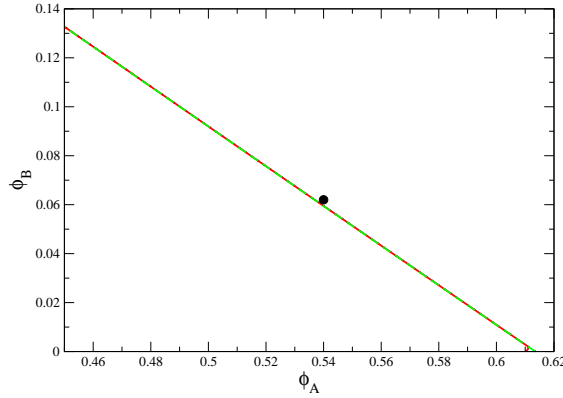


FIG. 5: This is the $\phi_C = 0.1$ plane. Note that all arrest lines have merged into one. The black dot finds itself in the non-ergodic region again.

The (ϕ_A, ϕ_C) plane

Now we will take a look at the (ϕ_A, ϕ_C) plane, where the particles B are found at infinite dilution (see Fig. 6). If we disregard the green dashed curve, which corresponds to the line of arrest of the particles B, the remaining curves correspond to a binary system with an asymmetry of $\delta_{CA} = \sigma_C/\sigma_A = 0.111$. This situation is quite analogous to the (ϕ_A, ϕ_B) plane of Figure 2, provided the same green dashed line is once more disregarded. Only the effect of the asymmetry is more important. Also, in a similar manner as we had before, there are two kinds of glasses made by the large particles. In the lower part of the red curve, the large particles form a repulsive glass whereas in the upper part they form an attractive glass. This time, however, the localization length of the large particles drops by five orders of magnitude. Another line of arrest, but not less important, corresponds to the localization of species B (dashed green line). It is worthwhile noting that although there is only one trace of them, their phase diagram is governed or strongly correlated with the species A (continued red line).

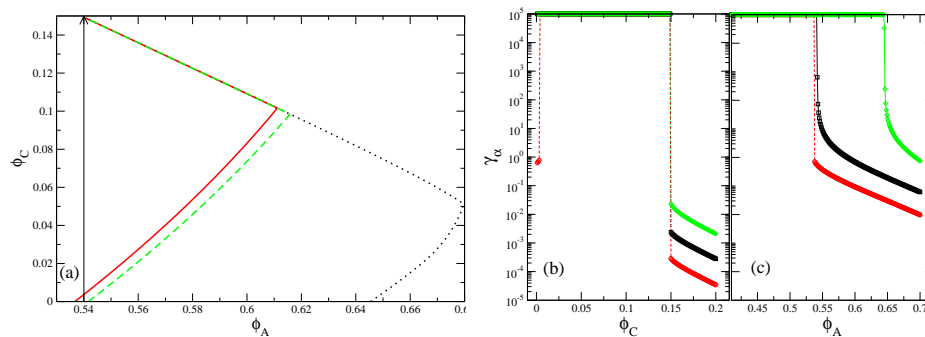


FIG. 6: (a) Plane $\phi_B = 0.0$, it shows the arrest lines of species A (red line), B (dashed green line) and C (black dotted line). (b) and (c) figures show the square localization lengths of particles of type A (red), B (black) and C (green) along the arrow drawn in figure (a) and along the ϕ_A axis, respectively. The units are the same of Fig 2.

CONCLUSIONS

In summary we have investigated the dynamic arrest phase diagrams of a ternary hard sphere mixture with relative sizes 1:3:9, and found that there is a glass-fluid-glass-fluid-glass transition of the bigger species. The first glass-fluid-glass is due the depletion forces caused by the presence of the middle particles and the second re-entrance as a result of adding an even smaller species. The full kinetic phase diagrams for the cases $\phi_C = 0.0$, $\phi_C = 0.05$, $\phi_C = 0.1$ and $\phi_B = 0$ were shown. We also shown the differences between MCT and SCGLE theories in the kinetic phase diagrams of a binary mixture of hard spheres with size asymmetry of 0.5. These differences are highly relevant for example when it is required to describe the properties of a polymer colloid mixture. And we saw clearly that the MCT theory is not consistent with such experimental results, for instance the best and most consistent description the SCGLE theory. In light of these results we conclude that the SCGLE theory is an excellent tool when we will try to describe systems with a high degree of polydispersity.

ACKNOWLEDGMENTS: This work was supported by PROMEP under grant PROMEP-103.5-11-4911.

-
- [1] C. A. Angell, *Science* **267**, 1924 (1995).
 - [2] P. G. Debenedetti and F. H. Stillinger, *Nature* **410**, 359 (2001).
 - [3] F. Mallamace *et al.*, *Phys. Rev. Lett.* **84**, 5431 (2000).
 - [4] S.-H. Chen *et al.*, *Science* **300**, 619 (2003).
 - [5] W. R. Chen *et al.*, *Phys. Rev. E* **68**, 041402 (2003).
 - [6] J. Grandjean and A. Mourchid, *Europhys. Lett* **65**, 712 (2004).
 - [7] D. Pontoni, S. Finet, T. Narayanan, A. R. Rennie, *J. Chem Phys.* **119**, 6157 (2003).
 - [8] K. N. Pham *et al.*, *Science* **296**, 104 (2002).
 - [9] K. N. Pham *et al.*, *Phys. Rev. E* **69**, 011503 (2004).
 - [10] W. Götze, in *Liquids, Freezing and Glass Transition*, edited by J. P. Hansen, D. Levesque, and J. Zinn-Justin
 - [11] J. Bergenholtz and M. Fuchs, *Phys. Rev. E* **59**, 5706 (1999).
 - [12] L. Fabbian *et al.*, *Phys. Rev. E* **59**, R1347 (1999); **60**, 2430 (1999).
 - [13] E. Zaccarelli *et al.*, *Phys. Rev. Lett.* **92**, 225703 (2004).
 - [14] R. Juárez-Maldonado and M. Medina-Noyola, *Phys. Rev. E* **77**, 051503 (2008).
 - [15] R. Juárez-Maldonado and M. Medina-Noyola, *Phys. Rev. Lett.* **101**, 267801 (2008).
 - [16] P.E. Ramírez-González *et al.*, *Rev. Mex. Física* **53**, 327 (2007).
 - [17] L. Yeomans-Reyna *et al.*, *Phys. Rev. E* **76**, 041504 (2007).
 - [18] R. Juárez-Maldonado *et al.*, *Phys. Rev. E* **76**, 062502 (2007).
 - [19] P. E. Ramírez-González *et al.*, *J. Phys.: Cond. Matter*, **20**: 20510 (2008).
 - [20] J. P. Hansen and I. R. McDonald, *Theory of Simple Liquids* (Academic Press Inc., 1976).
 - [21] G. Nägele, *Phys. Rep.* **272**, 215 (1996).
 - [22] M. A. Chávez-Rojó and M. Medina-Noyola, *Phys. Rev. E* **72**, 031107 (2005); *ibid* **76**, 039902 (2007).
 - [23] R. J. Baxter, *JCP* **52**, 4559 (1969)
 - [24] S. Asakura and F. Oosawa, *J. Polym. Sci.* **33**, 183 (1958).